

Pulse Radiolysis Studies on the Temperature-Dependent Spectrum and the Time-Dependent Yield of Solvated Electron in Propane-1,2,3-triol

Mingzhang Lin,[†] Haiying Fu,[‡] Isabelle Lampre,^{§,#} Vincent de Waele,^{§,#} Yusa Muroya,[‡] Yu Yan,[§] Shinichi Yamashita,[†] Yosuke Katsumura,^{*,†,§} and Mehran Mostafavi^{*,§,#}

Advanced Science Research Center, Japan Atomic Energy Agency, 2-4 Shirakata shirane, Tokaimura, Nakagun, Ibaraki 319-1195, Japan, Nuclear Professional School, School of Engineering, University of Tokyo, 2-22 Shirakata shirane, Tokaimura, Nakagun, Ibaraki 319-1188, Japan, Laboratoire de Chimie Physique/ELYSE, Université Paris-Sud 11, UMR 8000, Bât. 349, Orsay F-91405, CNRS, Orsay, F-91405, and Department of Nuclear Engineering and Management, School of Engineering, University of Tokyo, Hongo 7-3-1, Bunkyo-ku, Tokyo 113-8656, Japan

Received: June 3, 2009; Revised Manuscript Received: September 16, 2009

With a revisit of the absorption coefficient of the solvated electron in propane-1,2,3-triol, the temperature-dependent behavior of the absorption spectrum of solvated electron was studied from room temperature to 573 K by pulse radiolysis techniques. The change in the absorption spectrum of solvated electron in propane-1,2,3-triol observed by cooling down from a high temperature to 333 K is compared with that occurring during the electron solvation process at 333 K. The effect of the specific molecular structure of propane-1,2,3-triol compared to other alcohols is discussed.

Introduction

Five years ago we started to study the behavior of excess electrons in polyols.^{1–10} The solvation dynamics of excess electrons produced by two-photon solvent ionization and the temperature dependence of the absorption spectra of solvated electron generated by pulse radiolysis in ethane-1,2-diol (12ED, ethylene glycol), propane-1,2-diol (12PD), and propane-1,3-diol (13PD) were studied in parallel.

For the solvated electron formation, in 12ED, we observed that, at very short time after the pump pulse, the excess electron presents a very broad absorption band in the visible and near-infrared domain with a maximum around 675 nm. The red part of the absorption band drops rapidly for the first 5 ps while the blue part increases slightly, leading to a blue shift of the absorption band maximum down to 590 nm. Then, the absorbance on the red side of the spectrum follows its decrease while the absorbance on the blue side remains nearly constant. As a consequence, the maximum of the absorption band continues to shift toward shorter wavelengths and, 50 ps after the pump pulse, reaches 570 nm, that is, the position of the absorption band maximum of the equilibrated solvated electron in 12ED.⁹ We also investigated the formation of solvated electrons in two neat isomers of propanediol (PD).⁷ The excess electron in both 12PD and 13PD as in 12ED presents a wide absorption band in the visible and the near-IR at very short time delays after the pump pulse. The time-resolved spectra also revealed that a localized electron, which absorbs in the blue spectral domain, is quickly formed and relaxes to the equilibrated solvated

electron in a couple of tens of picoseconds. The electron solvation dynamics appear slower in 12PD than in 13PD.

As a concern of the temperature effect on the absorption band of excess electrons, in 12ED, the maximum of the absorption band shifts to the longer wavelength with increasing temperature, from 570 nm (2.17 eV) at room temperature to about 850 nm (1.46 eV) at 598 K. This red shift of -0.7 eV corresponds to a temperature coefficient of $dE_{\max}/dT = -2.4 \times 10^{-3} \text{ eV K}^{-1}$.¹⁰ Chandrasekhar et al.¹¹ reported a value of $(-2.49 \pm 0.07) \times 10^{-3} \text{ eV K}^{-1}$ (for $296 \text{ K} < T < 453 \text{ K}$), and at lower temperatures, Freeman et al.¹² determined a value of $-2.5 \times 10^{-3} \text{ eV K}^{-1}$. We observed that the behavior of solvated electrons in the two propanediols as a function of temperature is close. The transition energy at the absorption maximum plotted as a function of temperature is also correctly fitted by a straight line for both 12PD and 13PD.⁸ The temperature coefficient (dE_{\max}/dT) was found to be equal to $(-3.1 \pm 0.1) \times 10^{-3} \text{ eV K}^{-1}$ for 12PD and $(-2.80 \pm 0.06) \times 10^{-3} \text{ eV K}^{-1}$ for 13PD. At lower temperature, Freeman et al.¹² reported the values of -2.7×10^{-3} and $-3.0 \times 10^{-3} \text{ eV K}^{-1}$, respectively. Therefore, an average temperature coefficient of $(-2.9 \pm 0.1) \times 10^{-3} \text{ eV K}^{-1}$ and $(-2.80 \pm 0.04) \times 10^{-3} \text{ eV K}^{-1}$ could be assumed for 12PD and 13PD, respectively. Those latter values are very close to each other and higher than the values obtained in 12ED (around $-2.5 \times 10^{-3} \text{ eV K}^{-1}$).^{10,11} Nevertheless, as the length of the aliphatic chain and the number of hydroxyl groups are the same for both solvents, our observations emphasize the significant influence of the distance between the two $-\text{OH}$ groups on the behavior of the trapped electron. At room temperature, the energy of the absorption maximum is higher in 12PD than that in 13PD, and the absorption band of the solvated electron is narrower in 12PD than that in 13PD. These observations suggest that the two neighboring $-\text{OH}$ create deeper electron traps and a narrower distribution of traps in 12PD compared with 13PD. These results are in agreement with those reported for 12ED at high temperature and for 12ED and 13PD glasses. However, the traps in 12PD appear less deep

* Corresponding authors. E-mail: mehran.mostafavi@lcp.u-psud.fr (M.M.) and katsu@n.t.u-tokyo.ac.jp (Y.K.).

[†] Japan Atomic Energy Agency.

[‡] Nuclear Professional School, School of Engineering, University of Tokyo.

[§] Université Paris-Sud 11.

[#] CNRS.

[§] Department of Nuclear Engineering and Management, School of Engineering, University of Tokyo.

than those in 12ED since the energy of the absorption maximum of the solvated electron measured at a given temperature is lower in 12PD than to 12ED. That shows an influence of the additional methyl group on the solvent structure, in particular, on the created three-dimensional networks of hydrogen-bonded molecules. Nevertheless, it is to be noted that those considerations are indicative as the observed electron absorption band is the sum of three $s \rightarrow p$ transitions.

For the three solvents, we compared the time evolution of the absorption spectra of the excess electron with the temperature evolution of the absorption spectra of solvated electron. The electron absorption spectrum at any time during the relaxation process is identical to the spectrum of the solvated electron in the state of equilibrium with the solvent at some higher temperature. In this approach, the electron stabilization is viewed as a succession of quasi-equilibrium states that are fully characterized by the time evolution of the local temperature. The time-evolution of the absorption spectrum of the solvated electron can be accurately described by the temperature-dependent absorption spectrum of the ground state solvated electron suggesting that the spectral blue shift would be mostly caused by a continuous relaxation or "cooling" of the electron trapped in a solvent cavity.

More recently, the time-dependent absorption band of the photogenerated excess electron in propane-1,2,3-triol (123PT, glycerol) was reported.⁵ The molecular structure of 123PT which is a very high viscous solvent and presents a high hydrogen bond density, contains three hydroxyl groups in vicinity and completes the series of the polyols previously studied. Femtosecond photolysis measurements showed that, in the case of 123PT, in spite its higher viscosity, the excess electron is more quickly trapped and fully solvated than that in 12PD, 13PD, and 12ED. The small blue shift of the absorption band during solvation process highlights that the geometrical configuration of the pre-existing traps in 123PT is very close to that of fully solvated electrons. So, the solvation dynamics does not correlate to diffusion but depends on the molecular structure of the solvent, particularly on the density of OH groups that play an important role in the fast stabilization of the excess electron. The absorption spectrum of the solvated electron in 123PT has already been measured at different temperatures: Arai and Sauer recorded optical absorption spectra of e_s^- in 123PT and some 123PT/water mixtures at room temperature 298 K.¹³ The absorption spectra of the solvated electron in 123PT were also recorded at lower temperatures 76 and 195 K by Thomas et al.¹⁴ Later, Jou and Freeman measured a high quality spectrum of e_s^- in 123PT but only at 299 K.¹⁵ Recently, the spectrum of the solvated electron in propane-1,2,3-triol, generated by photodetachment from a halogen anion, between 329 and 536 K has been reported too.¹⁶

Nevertheless, to compare our results on solvation dynamics of electron in propane-1,2,3-triol⁵ with temperature-dependent absorption spectra, a larger temperature domain is needed. Moreover, some disagreements exist in the literature about the extinction coefficient of solvated electron and the time-dependent radiolytic yield at room temperature. Therefore, hereafter, we present a pulse radiolysis study in propane-1,2,3-triol to determine the extinction coefficient of the solvated electron and its radiolytic yield at room temperature as well as its absorption spectrum on a wide range of temperature from 298 to 573 K. Finally, we compare the spectral evolution of excess electron with time during solvation process and that of solvated electron with temperature. These results complete our data with different

polyols and help us also to reach a better description of solvation dynamics of electrons in these liquids.

Experimental Section

Propane-1,2,3-triol (123PT) and 4,4'-bipyridine (44Bpy) were purchased from Wako Pure Chemical Industries, Ltd., and used as received. The sample solutions were freshly prepared, deaerated by Ar gas for about 15 min, and then continuously purged with Ar gas above the surface during the measurements. Because of the low volatility of 123PT, the mass loss was negligible.

The nanosecond pulse radiolysis experiments were carried out at the University of Tokyo using a linear electron accelerator (energy, 35 MeV; pulse width, 10 ns) coupled with an absorption spectroscopic detection system. The trigger signals to the accelerator and the Xe pulse lamps and the change in the monochromator wavelength, as well as the data transfer from the oscilloscope were controlled by PCs through GPIB. A blocking filter at 340 nm was used to cut the scattered and multiple orders light for the wavelength range 340–520 nm while a filter at 520 nm was used for wavelength range 520–900 nm.

Room Temperature. The optical path length of the quartz cell was usually 20 mm. The dosimetry was done with a N_2O -saturated 10 mM KSCN aqueous solution, taking $G_{e((SCN)_2^{\cdot-})} = 5.2 \times 10^{-4} \text{ m}^2/\text{J}$ at 472 nm.¹⁷ Then, the absorbed dose, D , in 123PT was calculated by the equation $D_{123PT} = D_{H_2O} \times \rho_{123PT}$, where ρ_{123PT} stands for the density of 123PT. The dose fluctuations were less than 5% during a daylong experiment.

Pulse Radiolysis Measurements at High Temperature. The high temperature high pressure optical cell was made by Taiatsu Techno. The size of the irradiation cell was fairly compact so that it is easy to set up the optical detection system.¹⁸ High signal/noise ratios could be obtained because the effective diameter of the sapphire window for optical access was 6 mm and the optical path was 15 mm. The cell can withstand temperatures and pressures up to 400 °C and 40 MPa, respectively. We fixed the pressure at 10 MPa for all temperatures. Because of the extreme high viscosity of 123PT, the solution was heated in a water bath up to 363 K while bubbling with Ar gas, before being loaded to a syringe pump (Model 100DM) made by Teledyne Isco, Inc. The temperature of the sample solution was monitored by a thermocouple placed inside the cell and the pressure was adjusted with a back-pressure regulator.

Results and Discussion

Reactivity of e_{sol}^- in 123PT. Different concentrations of 44Bpy from 2 to 20 mM were used to scavenge the solvated electron in 123PT. The transient absorption monitored at 750 nm is mainly due to the solvated electron (inset in Figure 1). The decay of the solvated electron is accelerated by increasing the concentration of the scavenger because of the following reaction:



The anion $Bpy^{\cdot-}$ reacts very quickly with H^+ to form the neutral radical $BpyH^{\cdot}$.



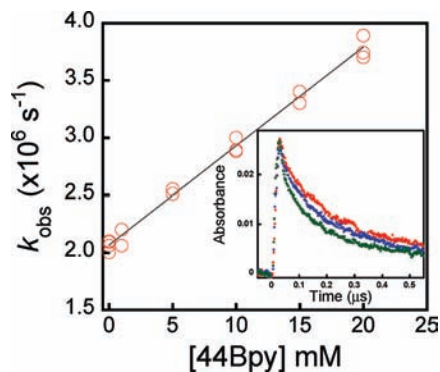


Figure 1. Pseudofirst order rate constant k_{obs} as a function as 44Bpy concentration. Inset: transient absorption signals at 750 nm recorded after nanosecond electron pulse in 123PT in the presence of different concentrations of 44Bpy.

The maximum of the absorption band of this neutral radical in 123PT is located at 530 nm, and the extinction coefficient in aqueous solution is known to be $13\,000\text{ M}^{-1}\text{ cm}^{-1}$.¹⁹ Because of high concentrations of 44Bpy, the kinetics follow pseudo-first order law with a rate constant $k_{\text{obs}} = k_1[44\text{Bpy}]$ (Figure 1). From the slope of k_{obs} versus $[44\text{Bpy}]$, a rate constant value of $(8.6 \pm 0.3) \times 10^7\text{ M}^{-1}\text{ s}^{-1}$ is obtained for k_1 . This value of k_1 is much smaller than the rates of 44Bpy toward e_{sol}^- in 12ED, 12PD, and 13PD, which are 1.3×10^9 , 6.4×10^8 , and $6.7 \times 10^8\text{ M}^{-1}\text{ s}^{-1}$, respectively (Table 1). The rate constant appears related to the viscosity η of the solvents. Then, in Figure 2 is plotted the rate constant k of the reaction between 44Bpy and e_{sol}^- in various polyols and water as a function of the reciprocal of the viscosity. There is a fairly good linear relationship between k and $1/\eta$. As known, the rate constant of a reaction in solution can be described by the Noyes equation:²⁰

$$\frac{1}{k} = \frac{1}{k_{\text{diff}}} + \frac{1}{k_{\text{react}}} \quad (3)$$

where k_{diff} is the diffusion-encounter rate constant and k_{react} is the reaction rate constant of the product formation from the encounter pair. When $k_{\text{react}} \gg k_{\text{diff}}$, so that $k \approx k_{\text{diff}}$, the reaction will occur on every encounter and is called near-diffusion controlled. k_{diff} can be given by the Smoluchowski equation:

$$k_{\text{diff}} = 4\pi(D_A + D_B)(r_A + r_B)N \quad (4)$$

D_i and r_i are the diffusion coefficient and the reaction radius of the reacting species “i”, respectively, and N is Avogadro’s number. According to Stokes–Einstein relation:

$$D_i = k_B T / (6\eta r_i) \quad (5)$$

With k_B the Boltzmann’s constant, T the absolute temperature, and η the solvent viscosity, the Stokes–Einstein–Smoluchowski equation becomes

$$k_{\text{diff}} = \frac{2RT(r_A + r_B)}{3\eta r_A r_B} \quad (6)$$

where R represents the gas constant. So, the good linear relationship between k_{diff} and $1/\eta$ in Figure 2 would imply that

the reaction of 44Bpy with e_{sol}^- is near-diffusion controlled. In particular, as diffusion is very slow in 123PT, we can assume that in this solvent $k_{\text{react}} \gg k_{\text{diff}}$.

Extinction Coefficient of e_{sol}^- in 123PT. Both solvated electron and 44BpyH⁺ absorb around 530 nm in 123PT. At short time, just after the pulse, the absorption at 530 nm is mainly due to the solvated electron while at longer time the absorption is related to 44BpyH⁺ formed through the reaction (2) and which is stable for tens of microseconds. Figure 3 shows the time profiles recorded at 530 nm in the presence of different concentrations of 44Bpy. At the highest concentrations (>100 mM), a slight increase at $t > 1\ \mu\text{s}$ is observed and attributed to the formation of 44BpyH₂⁺, as discussed in our previous paper.⁶

From the plateau observed at 530 nm (Figure 3) for a given quencher concentration $[44\text{Bpy}] \leq 100\text{ mM}$ or from the absorbance at $0.5\ \mu\text{s}$ when $[44\text{Bpy}]$ is higher than 100 mM, by assuming an extinction coefficient of $13\,000\text{ M}^{-1}\text{ cm}^{-1}$ for 44BpyH⁺ as in aqueous solutions, we can obtain the concentration of 44BpyH⁺ formed after the pulse. Figure 4 gives the formation yield of 44BpyH⁺ versus the scavenging power. That yield of 44BpyH⁺ matches the scavenging yield of solvated electrons.

At a concentration of 300 mM, almost all solvated electrons produced by the pulse are scavenged by 44Bpy. Therefore, we can deduce the extinction coefficient of the solvated electron. In fact, the absorbance at 530 nm (at time zero) in the absence and in the presence of 300 mM 44Bpy is 0.103 and 0.122 , respectively.

According to the Beer–Lambert’s law, we have

$$\frac{\epsilon(e_s^- \text{ at } 530\text{ nm})}{\epsilon(44\text{BpyH}^+ \text{ at } 530\text{ nm})} = \frac{A_{530\text{ nm}}(0\text{ mM})}{A_{530\text{ nm}}(300\text{ mM})} \quad (7)$$

then

$$\epsilon(e_s^- \text{ at } 530\text{ nm}) = \frac{13\,000 \times 0.103}{0.122} = 10\,980\text{ M}^{-1}\text{ cm}^{-1} \quad (8)$$

We may also estimate the $\epsilon(e_s^- \text{ at } 530\text{ nm})$ from the time profile of the solvated electron in pure 123PT. In this measurement, the dose per pulse measured using 10 mM KSCN is 11.5 Gy. The absorbance in 2 cm cell at 530 nm at 100 ns after the pulse in the absence of scavenger is 0.08. A rough estimation of the radiolytic yield of the solvated electron can be deduced from the curve in Figure 4: $G(e_s^-)$ at 100 ns after the pulse is $0.260\ \mu\text{mol J}^{-1}$. From the following relation

$$\begin{aligned} A_{530\text{ nm}}(100\text{ ns}) &= \epsilon(e_s^- \text{ at } 530\text{ nm}) \times 1 \times c \\ &= \epsilon(e_s^- \text{ at } 530\text{ nm}) \times 1 \times G(e_s^- \text{ at } 100\text{ ns}) \times D_{\text{H}_2\text{O}} \times \rho_{123\text{PT}} \end{aligned} \quad (9)$$

we deduce the value of the extinction coefficient,

$$\begin{aligned} \epsilon(e_s^- \text{ at } 530\text{ nm}) &= \frac{A_{530\text{ nm}}(100\text{ ns})}{(1 \times G(e_s^- \text{ at } 100\text{ ns}) \times D_{\text{H}_2\text{O}} \times \rho_{123\text{PT}})} \\ &= 10\,600\text{ M}^{-1}\text{ cm}^{-1} \end{aligned} \quad (10)$$

TABLE 1: Properties and Results Obtained for Four Polyols and Water

	$k(e_s^-+44\text{Bpy})/$ ($\text{M}^{-1}\cdot\text{s}^{-1}$)	$\eta^{25\text{ }^\circ\text{C}}/$ ($\text{mPa}\cdot\text{s}$)	dielectric constant	λ_{max} of e_s^-/nm	$\epsilon/\text{M}^{-1}\cdot\text{cm}^{-1}$	$G/\mu\text{mol}\cdot\text{J}^{-1}$	G at 200 $\text{ns}/\mu\text{mol}\cdot\text{J}^{-1}$	$dE/dT/\text{meV K}^{-1}$
12ED	1.3×10^9 ^a	16.1	41.4	570	9000 ± 500 ^a	0.43 (at 30 ps) ^a	0.17 ^a	-2.5 ^b
12PD	6.4×10^8 ^a	40.4	27.5	565	9700 ± 500 ^a	0.35 (at 100 ps) ^a	0.17 ^a	-2.9 ^c
13PD	6.7×10^8 ^a	39.4	35.1	575	10000 ± 500 ^a	0.38 (at 100 ps)	0.22 ^a	-2.8 ^c
123PT	8.6×10^7 ^d	934	42	530	10800 ± 500 ^d	0.37 (at 250 ps) ^e	0.16 ^d	-2.6 ^d
Water	2.9×10^{10}	0.89	78.4	720	18800 ± 500	0.44 (at 30 ps)	0.27	-2.3

^a From ref 4. ^b From ref 10. ^c From ref 8. ^d This work. ^e Unpublished results.

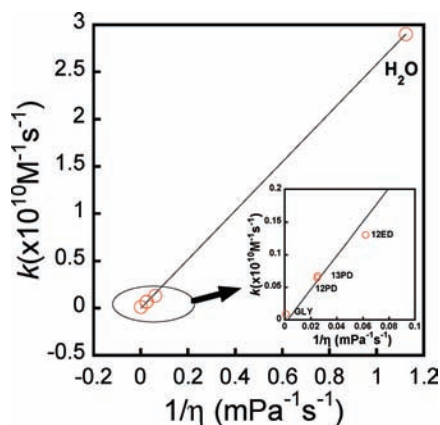


Figure 2. Rate constant k of the reaction between 44Bpy and solvated electron in different solvents as a function of the reciprocal of viscosity, $1/\eta$.

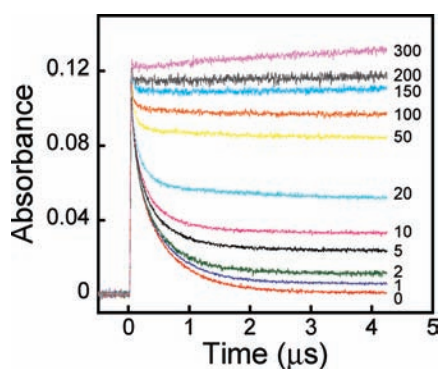


Figure 3. Time profiles recorded at 530 nm after nanosecond electron pulse in 123PT containing different concentrations of 44Bpy (in mM).

Within the errors, the values obtained by the two different methods are in good agreement. Therefore, we can assume that the extinction coefficient at the maximum of the absorption band is

$$\epsilon(e_s^- \text{ at } 530 \text{ nm}) = (10\,800 \pm 500) \text{ M}^{-1} \text{ cm}^{-1} \quad (11)$$

Uncertainties on this estimation are mainly due to the fluctuations of the dose per pulse and to the error on the value of the extinction coefficient of 44BpyH[•]. As electrons in 123PT are solvated in a few tens of picoseconds, to significantly scavenge electron precursor, for the highest concentration used in this work, the reaction rate constant between 44Bpy and electron precursor should be at least 5000 times higher than k_1 . Rate constant higher than $10^{12} \text{ L mol}^{-1} \text{ s}^{-1}$ are known for reactions of precursors that are more mobile than solvated electrons. But in this work, as the rate constant is not known, we assume that the scavenging of presolvated electron by 44Bpy is negligible. If the presolvated electrons are scavenged by 44Bpy, the value

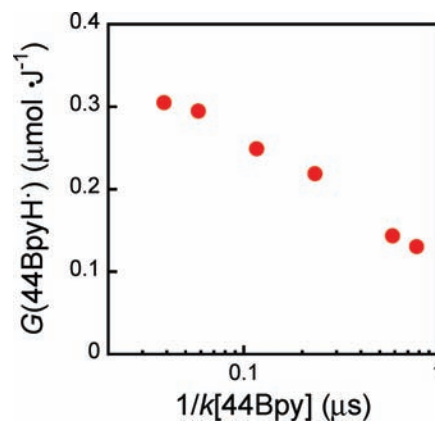


Figure 4. Yield of 44BpyH[•] radical as a function of scavenging time in 123PT.

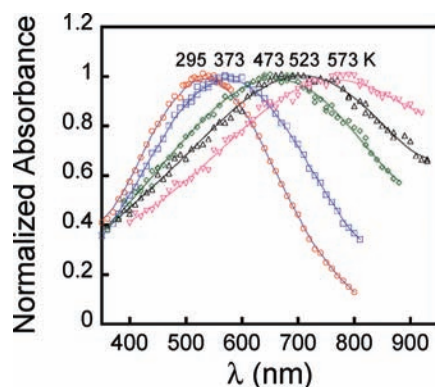


Figure 5. Normalized absorption spectra of the solvated electron in 123PT at different temperatures. The pressure was fixed at 10 MPa.

($10,800 \pm 500$) $\text{M}^{-1} \text{ cm}^{-1}$ should be corrected to a lower value. The found ϵ value is in fairly good agreement with that suggested by Jay-Gerin et al. from the values of the radiolytic yield of the solvated electron, $10\,500 \text{ M}^{-1} \text{ cm}^{-1}$,²¹ but lower than that usually reported of $12\,000 \text{ M}^{-1} \text{ cm}^{-1}$.¹⁴ According to our previous work on 12ED, 12PD, and 13PD, we assume that the lower value of the extinction coefficient is more accurate.

Temperature-Dependent Absorption Spectra e_s^- in 123PT.

Figure 5 shows the normalized absorption spectra of e_s^- in 123PT at 295, 373, 473, 523, and 573 K at a fixed pressure of 10 MPa. At $T > 573$ K, the decay becomes too fast, and the absorbance decreases too much, so that no reliable data can be obtained. As expected from previous results in other alcohols, the spectra shift to longer wavelength with increasing temperature. At room temperature, the absorption maximum is located around 530 nm, which agrees very well with reported data.^{22,23} The absorption bands (normalized in intensity and shifted in energy) for 4 temperatures between 300 and 600 K show that the shape of the absorption band hardly changes with increasing temperature (Figure 6). Some broadening on the blue side compared with the shape at lower temperature is observed at higher temperatures.

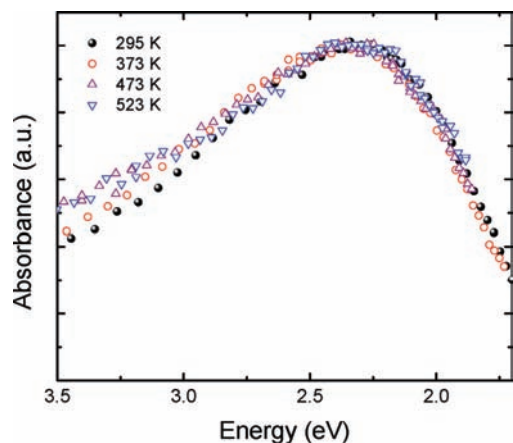


Figure 6. Normalized optical absorption spectra of the solvated electron at different temperatures shifted to the same maximum at 2.32 eV. The pressure was fixed at 10 MPa.

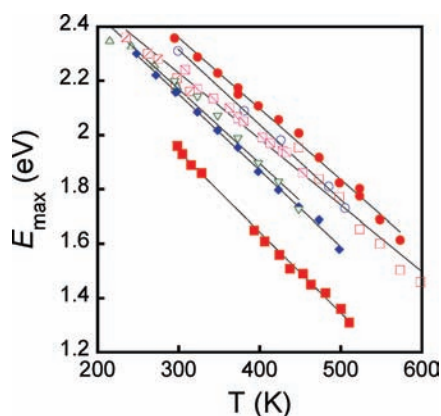


Figure 7. Absorption maxima of solvated electrons in various alcohols: (■) methanol, (●) propane-1,2,3-triol, this work; (○) propane-1,2,3-triol, from ref 16; (□) 12ED from ref 10; (▽) 12PD from ref 8; (◆) 13PD from ref 8.

Figure 7 shows the absorption maxima (E_{\max}) of e_s^- in various alcohols as a function of temperature. In the experimental temperature and pressure conditions, all of the data sets show fairly good linear relationship between E_{\max} and temperature in Kelvin. The curve with solid circles corresponds to the present work and leads to a temperature coefficient of $(-2.62 \pm 0.03) \times 10^{-3}$ eV/K. Obviously, the obtained data of E_{\max} are globally higher than those reported by Chandrasekhar, et al., but the found temperature coefficient dE_{\max}/dT is only slightly higher than their value, $(-2.67 \pm 0.07) \times 10^{-3}$ eV/K.¹⁶ It is to be noted that Chandrasekhar et al. measured the absorption spectra of the solvated electron by flash photolysis of KI in 123PT, and not in pure 123PT solvent. In fact, the absorption spectra of e_s^- in 123PT at 333 K measured by multiphoton ionization processes presents also a slightly shifted maximum (higher E_{\max} or lower wavelength (10 nm)) than that reported by Chandrasekhar et al. It is worth noting that the found value of dE_{\max}/dT is lower in absolute value than those given for 12ED, 12PD, and 13PD or for methanol (-3×10^{-3} eV/K; Table 1). This indicates that the temperature has a weak effect on the structure of the solvated electron in 123PT compared with other studied alcohols. With increasing the temperature, the density of the $-OH$ groups still remains high, and the traps remain deep enough to stabilize the excess electron well. The spectral properties of solvated electron in 123PT between 76 and 305 K suggested also that, even when the 123PT is highly hydrogen

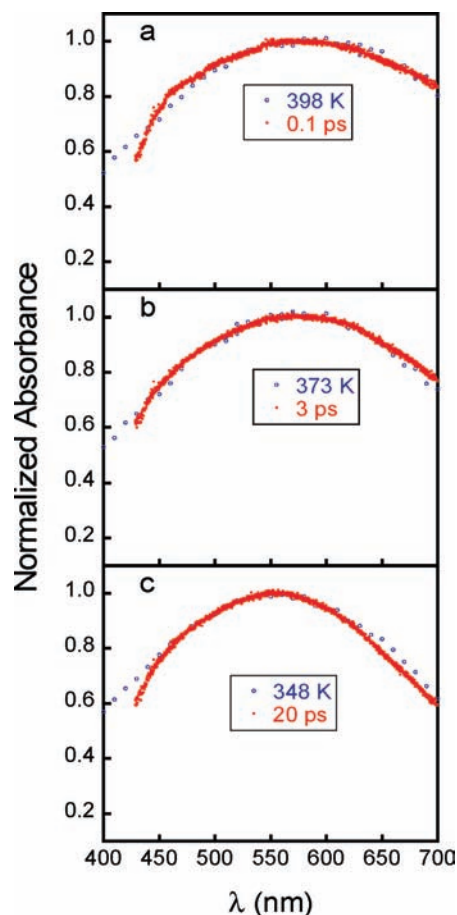


Figure 8. Comparison between the absorption spectra of the solvated electron obtained in 123PT by pulse radiolysis at different temperatures and those recorded at different times by laser photolysis at 333 K. The data concerning the time-resolved spectra during solvation dynamics are extracted from ref 5.

bounded at low temperature, many OH groups remain free to quickly trap the electron compared with other alcohols.¹⁴

Electron Solvation Dynamics and the Cooling Process of the High Temperature Solvated Electron. As mentioned in the introduction, we previously obtained the solvation dynamics of electrons in four polyols by femtosecond laser photolysis.^{1-3,5,7} From these studies, we found that the solvation dynamics is better described by a continuous relaxation model rather than by stepwise mechanisms involving different species. Indeed, during the solvation process at a given temperature, solvent molecules become organized around the excess electron. In the diols, this rearrangement appears similar to the one occurring during the solvent cooling down from a higher temperature to the given temperature; with the decrease in temperature, the cavity of the electron changes, becoming more compact and better organized.^{2,7} Such a time-dependent analogy had already been noticed for water too.²⁴ It should be remembered that for 123PT, due to its very high viscosity, the solvation dynamics process experiments were not performed at room temperature but at 333 K.⁵ So, the transient spectra recorded at 333 K after the photoionization of 123PT are compared with those of the solvated electron in the equilibrated state obtained here at higher temperatures by nanosecond pulse radiolysis. Figure 8 clearly show that the time-resolved spectrum recorded at 0.1, 3, and 20 ps after the laser pulse are similar to those obtained at 398, 373, and 348 K, respectively. For comparison, in the case of 12ED (12PD) the transient spectra recorded at 1 and 5 ps (1 and 4 ps) after the solvent photoionization at room temperature

are similar to the spectra of the solvated electron in the equilibrated state at higher temperatures, 448 and 373 K (423 and 373 K), respectively.^{2,7} These results show that in the case of 123PT the trapping and cooling process is very fast and confirm a comparable organization disorder of the solvent (increasing with T or as t tends to 0). In our experimental conditions, the solvation process appears as a continuous process indicating that the photogenerated electrons are rapidly trapped, with a characteristic time shorter than our temporal resolution and that the observed electrons are only localized electrons. In addition, we have observed a faster “cooling” for the trapped electrons in 123PT compared with 13PD and 12PD, in agreement with the solvation times obtained shorter in 123PT than in PD.

In summary, this paper deals with the solvated electron in propane-1,2,3-triol (glycerol). By using the scavenging method, the molar extinction coefficient has been determined to be $10\,800 \pm 500 \text{ L mol}^{-1} \text{ cm}^{-1}$ at 530 nm, the band maximum at room temperature. As expected, with increasing temperature, the absorption spectrum of solvated electron shifts to longer wavelengths. The temperature coefficient, dE_{max}/dT , is found to be $-2.6 \times 10^{-3} \text{ eV/K}$, a value intermediate between those obtained for 12ED ($-2.5 \times 10^{-3} \text{ eV/K}$) and PD ($-2.9 \times 10^{-3} \text{ eV/K}$ and $-2.8 \times 10^{-3} \text{ eV/K}$ for 12PD and 13 PD, respectively). The time-dependent spectra recorded at 333 K by femtosecond laser photolysis measurements during electron solvation match the temperature-dependent spectra of solvated electron, showing that electrons are trapped in less than 200 fs, the temporal resolution. Those results indicate that the geometrical configuration of the electron traps does not depend much on temperature and time, and suggest the presence of well-defined pre-existing electron traps in 123PT.

Acknowledgment. We are grateful to Mr. T. Ueda, Mr. K. Yoshii, and Professor M. Uesaka for their technical assistance in experiments and encouragement.

References and Notes

- (1) Lampre, I.; Pernot, P.; Bonin, J.; Mostafavi, M. *Radiat. Phys. Chem.* **2008**, *77*, 1183.
- (2) Bonin, J.; Lampre, I.; Pernot, P.; Mostafavi, M. *J. Phys. Chem. A* **2007**, *111*, 4902.
- (3) Lampre, I.; Bonin, J.; Soroushian, B.; Pernot, P.; Mostafavi, M. *J. Mol. Liq.* **2008**, *141*, 124.
- (4) Lin, M. Z.; Mostafavi, M.; Muroya, Y.; Lampre, I.; Katsumura, Y. *Nucl. Sci. Tech.* **2007**, *18*, 2.
- (5) Bonin, J.; Lampre, I.; Pernot, P.; Mostafavi, M. *J. Phys. Chem. A* **2008**, *112*, 1880.
- (6) Lin, M. Z.; Mostafavi, M.; Muroya, Y.; Han, Z. H.; Lampre, I.; Katsumura, Y. *J. Phys. Chem. A* **2006**, *110*, 11404.
- (7) Soroushian, B.; Lampre, I.; Bonin, J.; Pernot, P.; Pommeret, S.; Mostafavi, M. *J. Phys. Chem. A* **2006**, *110*, 1705.
- (8) Lampre, I.; Lin, M.; He, H.; Han, Z.; Mostafavi, M.; Katsumura, Y. *Chem. Phys. Lett.* **2005**, *402*, 192.
- (9) Soroushian, B.; Lampre, I.; Pommeret, S.; Mostafavi, M. “Solvation dynamics of electron in ethylene glycol at 300 K” in *Femtochemistry And Femtobiology: Ultrafast Events In Molecular Science*; Martin, M. M., Hynes, J. T., Eds.; Elsevier Science: New York, 2004; p 241.
- (10) Mostafavi, M.; Lin, M.; He, H.; Muroya, Y.; Katsumura, Y. *Chem. Phys. Lett.* **2004**, *384*, 52–55.
- (11) Chandrasekhar, N.; Krebs, P. *J. Chem. Phys.* **2000**, *112*, 5910–5914.
- (12) Okazaki, K.; Idrissali, K. M.; Freeman, G. R. *Can. J. Chem.-Rev. Can. Chim.* **1984**, *62*, 2223.
- (13) Arai, S.; Sauer, M. C., Jr. *J. Chem. Phys.* **1966**, *44*, 2297.
- (14) Kajiwara, T.; Thomas, J. K. *J. Chem. Phys.* **1972**, *76*, 1700.
- (15) Jou, F.-Y.; Freeman, G. R. *Can. J. Chem.* **1979**, *57*, 591. Jou, F.-Y.; Freeman, G. R. *J. Phys. Chem.* **1979**, *83*, 261.
- (16) Chandrasekhar, N.; Krebs, P.; Unterreiner, A. N. *J. Chem. Phys.* **2006**, *125*, 164512.
- (17) Buxton, G. V.; Stuart, C. R. *J. Chem. Soc., Faraday Trans.* **1995**, *91*, 279.
- (18) Mostafavi, M.; Lin, M. Z.; Wu, G. Z.; Katsumura, Y.; Muroya, Y. *J. Phys. Chem. A* **2002**, *106*, 3123.
- (19) Simić, M.; Ebert, M. *Int. J. Radiat. Phys. Chem.* **1971**, *3*, 259.
- (20) Noyes, R. M. *Prog. React. Kinet.* **1961**, *1*, 131.
- (21) Jay-Gerin, J. P.; Ferradini, C. *J. Chim. Phys.* **1994**, *91*, 173.
- (22) Dorfman, L. M.; Jou, F. Y. “Optical absorption spectrum of the solvated electron in ethers and in binary liquid systems.” In *Electrons in Fluids*; Jortner, J., Kestner, N. R., Eds.; Springer: New York, 1972; p 447.
- (23) Jou, F. Y.; Freeman, G. R. *Can. J. Chem.* **1979**, *59*, 591.
- (24) Lian, R.; Crowell, R. A.; Shkrob, I. A. *J. Phys. Chem. A* **2005**, *109*, 1510.

JP905199D